Ninth International Conference on Computational Fluid Dynamics (ICCFD9), Istanbul, Turkey, July 11-15, 2016 **ICCFD9-124**

ENATE procedure for the Navier-Stokes equations

Antonio Pascau[1], Müslüm Arıcı[2], Víctor Llorente[1]

[1] Fluid Mechanics Group and LIFTEC, University of Zaragoza and CSIC, Zaragoza 50018, Spain
[2] Mechanical Enginering Department, Umuttepe Campus, Kocaeli University, Kocaeli 41380, Turkey

Corresponding author: pascau@unizar.es

Abstract: This paper presents novel results in the application of the ENATE procedure to the Navier Stokes equations in 1D. ENATE procedure can deal with sources of various kinds, in particular, discontinuous sources (with discontinuous derivatives of any order) or even sources of delta Dirac type. It always provides solutions of very high accuracy with relatively few nodes compared to other high-precision schemes whose performance is very much dependent on the particular numerical example chosen.

Keywords: Numerical Algorithms, Computational Fluid Dynamics, ENATE procedure.

1 Introduction

There are plenty of physical phenomena governed by transport equations. This kind of Partial Differential Equations (PDE) appears in many branches of science, in particular Fluid Mechanics. The values that certain variable attains in the domain are those that satisfy a balance between convection and diffusion processes and source, if any. Exact solutions of these equations are difficult to obtain, normally requiring assumptions on the coefficients, so in order to know the problem one has to resort to numerical techniques that provide an approximate solution.

A wide choice of numerical schemes to obtain the flow field, have been developed along the years such as finite differences, finite elements, finite volumes, or spectral. Although these approaches get the numerical solution in a relatively short time, a lot of neighbour data[1] needs to be handled for precise results. For a standard discretization it is worth pointing out that none of these methods uses the solution of the ODE that can be obtained if the multidimensional PDE is integrated over an interval along a given coordinate. As a result of this integration the PDE converts into an nonhomogeneous first-order ODE whose solution can be written in terms of its homogeneous and particular solutions via the general theory of first-order ODEs. The ENATE procedure has shown to provide very accurate and robust solutions to problems governed by transport equations of any kind [1, 2] with a very narrow computational molecule of only three points. The first application of this procedure was presented at the 6th ICCFD International Conference in Saint Petersburg in 2010. Since then an ample set of different applications has shown that the accuracy with very few nodes is higher than state-of-the-art high-order discretizations. ENATE uses the exact solution of

[1]CFDers employ the word "computational molecule" to denote the discrete neighbour points algebraically related to a generic internal node.

the second-order Ordinary Differential Equations (ODE) (1) to derive an algebraic equation between nodes whose coefficients are integrals in a unity domain of reference.

$$\frac{d}{dx}\left(\rho u(x)\phi - \Gamma(x)\frac{d\phi}{dx}\right) = S(x) \tag{1}$$

For several dimensions the derivatives in other directions are required to be treated as pseudo-source. Apart from the first application of ENATE to the 1D Navier-Stokes equations presented in this paper, work is underway to extend ENATE to multidimensional problem along different approaches.

The paper is organized as follows; in Section 2 a brief review of the mathematical model [1, 2] is written down and in Section 3 the problem and the equations to be discretized are presented. In Section 4 some test cases are assessed and their numerical results plotted to show the performance of ENATE. Lastly, conclusions are provided in Section 5.

2 Theoretical Background

ENATE approach for the 1D convection-diffusion equation uses the integral solution of Equation (2) in normalized variables, Equation (3), for later making up an algebraic equation with the nodal values of the discretized problem. The domain is split in N intervals which may be equal length or not, and $N+1$ nodes with locations x_i, $i = 0, ..., N$, with two nodes at the boundaries, x_0 and x_N. lb and rb stands for left boundary and right boundary respectively. A normalized coordinate $\widehat{x}$ is chosen as independent variable by considering a mapping between the working interval of length $L = x_{rb} - x_{lb}$, and a unity domain, $x = x_{lb} + L\widehat{x}$, $0 \leqslant \widehat{x} \leqslant 1$, $x \in [x_{lb}, x_{rb}]$. The normalized equation is

$$\frac{d}{d\widehat{x}}\left(\widehat{\rho\upsilon}\widehat{\phi} - \frac{\widehat{\Gamma}}{P_{L0}}\frac{d\widehat{\phi}}{d\widehat{x}}\right) = -\frac{\phi_{lb}}{\Delta\phi}\frac{d\widehat{\rho\upsilon}}{d\widehat{x}} + \Pi_s \quad \text{with} \quad \Pi_s = \frac{S(\widehat{x})L}{(\rho\upsilon)_{lb}\Delta\phi} \tag{2}$$

$$\widehat{\phi} = \frac{\phi - \phi_{lb}}{\phi_{rb} - \phi_{lb}} = \frac{\phi - \phi_{lb}}{\Delta\phi} \quad ; \quad \widehat{\rho\upsilon} = \frac{\rho\upsilon}{(\rho\upsilon)_{lb}} \quad ; \quad \widehat{\Gamma} = \frac{\Gamma}{\Gamma_{lb}} \quad ; \quad P_{L0} = \frac{(\rho\upsilon)_{lb}L}{\Gamma_{lb}} \quad ; \quad \widehat{\lambda} = \frac{\widehat{\rho\upsilon}}{\widehat{\Gamma}} \tag{3}$$

By the well-known mathematical theory of ODEs, one can split the complete solution into a homogeneous part $\overline{\phi}^N(\widehat{x})$ and a particular part $F(\widehat{x})$ in such a way that the complete solution takes the expression $\widehat{\phi} = F(\widehat{x}) + (1 - F(1))\,\overline{\phi}^N(\widehat{x})$.

The link between two successive intervals is the value of the diffusive flux at the shared edge. This flux should be equal considering the edge to belong to either interval. The diffusive flux at a generic node P is calculated by considering it as the end point of one interval, WP, between the West node and P, or the start point of the next one, PE, between P and the East node. The final algebraic equation is as follows:

$$\begin{aligned}
&\left[(\rho\upsilon)_W\,\widetilde{k}_{WP} + (\rho\upsilon)_P\left(\widetilde{k}_{PE} + \left.\frac{ILE_{01}}{IGE_{01}}\right|_{PE}\right)\right]\phi_P = \\
&(\rho\upsilon)_W\left(\widetilde{k}_{WP} + \left.\frac{ILE_{01}}{IGE_{01}}\right|_{WP}\right)\phi_W + (\rho\upsilon)_P\,\widetilde{k}_{PE}\,\phi_E \\
&+ IS_{01}|_{WP} \\
&+ \left(\left.\frac{ISGE_{01}}{IGE_{01}}\right|_{PE} - \left.\frac{ISGE_{01}}{IGE_{01}}\right|_{WP}\right)
\end{aligned} \tag{4}$$

The different factors that appear in the formulation are

$$
\begin{aligned}
ILE_{01} &= \int_0^1 \frac{\widehat{\lambda}}{\overline{\overline{E}}} d\widehat{x}' \quad ; \quad IGE_{01} = \int_0^1 \frac{d\widehat{x}'}{\widehat{\Gamma}\overline{\overline{E}}} \quad ; \quad \widetilde{k} = \frac{1}{P_{L0} IGE_{01}} \\
ISGE_{01} &= \int_0^1 \frac{IS_{0\widehat{x}'}}{\widehat{\Gamma}\overline{\overline{E}}} d\widehat{x}' = \int_0^1 \frac{L \int_0^{\widehat{x}'} S(\widehat{x}'') d\widehat{x}''}{\widehat{\Gamma}\overline{\overline{E}}} d\widehat{x}' \\
IS_{01} &= L \int_0^1 S(\widehat{x})\, d\widehat{x} = \int_{x_{lb}}^{x_{rb}} S(x)\, dx
\end{aligned} \tag{5}
$$

Note that the two factors related to the source term, $ISGE_{01}$ and IS_{01}, are dimensional whereas those participating in the nodal coefficients, IGE_{01}, ILE_{01} and $\widetilde{k}$, are dimensionless. All integrals are between zero and one. They are evaluated by approximating the integrand by Hermite polynomials, given its values and derivatives at the edges of the reference interval. ENATE provides an algebraic relation between three nodes that is exact as long as the integrals have an analytical primitive. As this will not be generally the case the integrands must be numerically approximated.

3 Problem Statement

ENATE 1D approach solves the one-dimensional flow governed by the system of two equations related to mass conservation and momentum transport (N-S) for two unknowns: pressure and velocity. This flow, although simple, contains all essential features of the pressure-velocity coupling.

$$
\frac{d}{dx}\rho u = \dot{m} \tag{6}
$$

$$
\frac{d}{dx}\left(\rho u u - \mu \frac{du}{dx}\right) = -\frac{dP}{dx} + \dot{m}u + S_m \tag{7}
$$

These equations govern the motion of an incompressible 1D flow with mass and momentum injection such as that happening in fuel cells, where the mass suffers variations along the channel due to diffusion in the porous layer in the direction perpendicular to the serpentine channel that feeds the fuel (usually hidrogen) and air into the fuel cell. ρ may be considered as a line density (kgr/m) and $\dot{m}$ represents the mass source ($kgr/m/s$ injected to or extracted from the 1D domain) which may depend on x. In the Navier-Stokes equation the momentum source is $\dot{m}u$ as each $kgr/m/s$ of fluid injected/extracted at one point has to bring in/take away $\dot{m}u$ momentum units per meter, otherwise the variable u would have two different values at the same point. S_m represents additional momentum sources due to gravity forces and other body forces in non-inertial reference frames, if any.

The ENATE procedure for the Navier-Stokes equations transforms the original equation into:

$$
(\rho u)_P - (\rho u)_W = \int_W^P \dot{m}\, dx \tag{8}
$$

$$
P_P - P_W = (\rho u^2)_P - (\rho u^2)_W + \left(\frac{\mu}{\rho}\dot{m}\right)_P - \left(\frac{\mu}{\rho}\dot{m}\right)_W + \int_W^P \dot{m}u\, dx + \int_W^P S_m\, dx \tag{9}
$$

4 Numerical Tests

In this section numerical results are compared to the exact solutions in several test cases. By adjusting appropriately the source terms a wealth of different (continuous and discontinuous) analytic solutions may be obtained, in the same way as in Pascau [3]. All physical properties have been taken as constants of value one and the inlet conditions are $u_0 = 1$ and $p_0 = 0$. On the whole, a continuous solution for (6) and (7) can be read as

$$u(x) = u_0 + \frac{1}{\rho}\int_{x_0}^{x} \dot{m}(x)dx \tag{10}$$

$$P(x) = P_0 + \frac{\mu}{\rho}\left(\dot{m}(x) - \dot{m}_0\right) + \int_{x_0}^{x}\left(S_m(x) - \dot{m}(x)\left[u_0 + \frac{1}{\rho}\int_{x_0}^{x}\dot{m}(x)dx\right]\right)dx \tag{11}$$

Four tests cases were worked out in a domain $\Omega \in [0, 1]$ where $\dot{m}$ and S_m were discontinuous. In the interval $[0, 0.3)$ there were no sources present, whereas mass and momentum source were activated within $(0.3, 0.7)$. From 0.7 onwards the mass source was constant taking the same value as in 0.7 , and the momentum source was zero. Further, either $\dot{m}$ or S_m adopted different mathematical expressions in the second interval to produce several test cases whose results are written down in the next subsections. Additionally, the mass extraction produces a jump in the second derivative of the velocity and consequently in the pressure, at each side of the discontinuity.

$$\int_{x^-}^{x^+} \mu\frac{d^2u}{dx^2}dx = \int_{x^-}^{x^+} A\delta(x - x_d)dx = A \quad \text{with} \quad A = \frac{\mu}{\rho}\dot{m} \tag{12}$$

where x_d denotes the discontinuity point and x^+/x^- are right/left side at x_d. In order to perform Hermite interpolation for the integral of $\dot{m}u$ in Equation (9) a set of values and derivatives at nodal points (W,P) are required. Being ρu known by Equation (8), every single integral can be evaluated through Equation (6). Here, a list of the derivatives is shown for completeness:

- Cubic Hermite (4th Order)

$$\left.\frac{d(\dot{m}u)}{dx}\right|_{W,P} = (u)_{W,P}\left.\frac{d\dot{m}}{dx}\right|_{W.P} + \left.\frac{\dot{m}^2}{\rho}\right|_{W,P}$$

- Quintic Hermite (6th Order)

$$\left.\frac{d^2(\dot{m}u)}{dx^2}\right|_{W,P} = (u)_{W,P}\left.\frac{d^2\dot{m}}{dx^2}\right|_{W.P} + \left.\frac{3\dot{m}}{\rho}\right|_{W,P}\left.\frac{d\dot{m}}{dx}\right|_{W,P}$$

- Septic Hermite (8th Order)

$$\left.\frac{d^3(\dot{m}u)}{dx^3}\right|_{W,P} = (u)_{W,P}\left.\frac{d^3\dot{m}}{dx^3}\right|_{W.P} + \left.\frac{4\dot{m}}{\rho}\right|_{W,P}\left.\frac{d^2\dot{m}}{dx^2}\right|_{W,P} + \left.\frac{3}{\rho}\left(\frac{d\dot{m}}{dx}\right)^2\right|_{W,P}$$

4.1 $\dot{m}$ linear and S_m linear

In the first case, $\dot{m}$ and S_m were linear in the active interval

$$\dot{m} = \dot{m}_0 \frac{x - 0.3}{0.7 - 0.3} \quad ; \quad S_m = S_{m0} \frac{x - 0.3}{0.7 - 0.3}$$

where $\dot{m}_0$ and S_{m0} are both equal to 100. We chose this value in order to test how good or bad is the numerical approach with a steep slope in both sources. As we can see in Fig.1, these high slopes affect more the exact pressure than the velocity, the former turns into high negative values in some zones.

Regarding the numerical results, we got machine accuracy for both velocity and pressure for a small number of nodes, 10. For all interval lengths the energy norm is the same, so L_2 vs Δx is not plotted for neither Hermite polynomial.

4.2 $\dot{m}$ linear and S_m exponential

In this case $\dot{m}$ is linear as well but with $\dot{m}_0 = 1$. The mass source was very simple, inasmuch as an exponential momentum source was intended to be checked. The function that defines both is

$$\dot{m} = \frac{x - 0.3}{0.7 - 0.3} \quad \text{with} \quad S_m = e^{5x}$$

In Fig.2, norms for the discretization errors of the velocity/pressure field were plotted. As expected, the energy norm for the velocity gets machine accuracy with just 10 nodes, as in the previous case. This happens due to the velocity dependence on $\dot{m}$ only, hence S_m does not play a role in its accuracy.

Regarding the order of convergence, the Hermite polynomials provide what the theory predicts: 4th order for Cubic, 6th order for Quintic and 8th order for Septic. In the worst case, L_2 takes a value around 10^{-13} with 10,000 nodes, which is near machine accuracy. The comparison between exact and numerical solutions is shown in Fig.3.

4.3 $\dot{m}$ exponential and S_m linear

Tests 4.1 and 4.2 gave goods results for velocity, and also for pressure. So, in the next two cases a combination of $\dot{m}$ exponential and S_m linear or exponential was established. The mass/momentum sources read

$$\dot{m} = e^{5x} - e^{1.5} \quad \text{with} \quad S_m = \frac{x - 0.3}{0.7 - 0.3}$$

L_2 vs Δx is shown in Fig.4 and exact solution vs numerical solution in Fig.5. Energy norm values are a bit worse than in the previous case. For the pressure and with $\Delta x = 10^{-2}$, values of 10^{-6}, 10^{-10} and 10^{-13} are found, to be compared with $5 \cdot 10^{-7}$, 10^{-12} and 10^{-15} in 4.2. This worsening of the L_2 is caused by the integral of $\dot{m}u$, which is a dominant source term in the pressure Equation (9). Something slightly different is found in the velocity. To reach machine accuracy more than 10 nodes are required because the exponential of S_m is not appropriately interpolated and hence, the integrand not accurately calculated. The order of convergence is that expected.

4.4 $\dot{m}$ exponential and S_m exponential

Finally, for solutions where both mass and momentum source were exponential

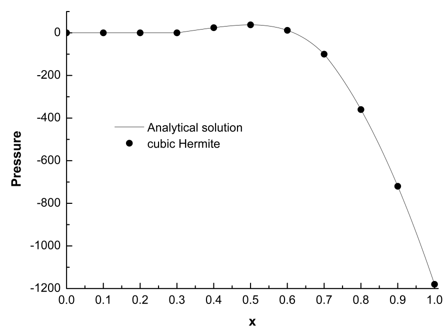

(a) Pressure field.

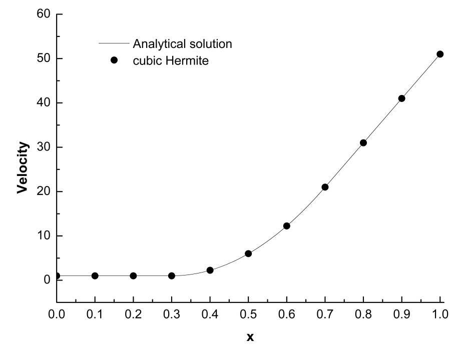

(b) Velocity field.

Figure 1: Case $\dot{m}$ and S_m linear. Exact solution vs numerical solution with 9 internal nodes and 2 boundary nodes.

$$\dot{m} = e^{5x} - e^{1.5} \quad \text{with} \quad S_m = e^{10x}$$

There is change in the factor of the exponential of S_m. The exact and numerical results were plotted in Fig.7. As we can see in Fig.6, the results are not different from the previous case. Only for the pressure there were a slightly deterioration of his energy norm.

5 Conclusion and Future Work

ENATE is a procedure designed to obtain an algebraic equation that links nodal values of a convection-diffusion equations. Under this idea, the discretization reduces to a numerical integration problem, instead of a numerical differentiation problem. The numerical errors introduced in the integral evaluation are considerably less than those obtained when dealing with approximation methods of the derivatives. With regard to the case tested, it was found that the mass source plays a more important role in eqns.(8)-(9) than the momentum source. Even with exponential sources ENATE provides solutions close to machine accuracy with a small number of nodes.

An obvious extension of ENATE 1D are The Navier Stokes equations in 2D. These introduce additional difficulties as the derivatives in other directions have to be considered as pseudo-sources. Work is underway o accommodate ENATE in 2D.

References

[1] A. Pascau. An exact discretization for a transport equation with piecewise-constant coefficients and arbitrary source. *Comput Fluids,*, 75:42–50, 2013.

[2] A. Pascau and M. Arici. An accurate discretization for an inhomogeneous transport equation with arbitrary coefficients and source. *Comput Fluids,*, 125:101–115, 2016.

[3] A. Pascau. Cell face velocity alternatives in a structured colocated frid for the unsteady Navier-Stokes equations. *Int. J. Numer. Meth. Fl.*, 65(7):812–833, 2011.

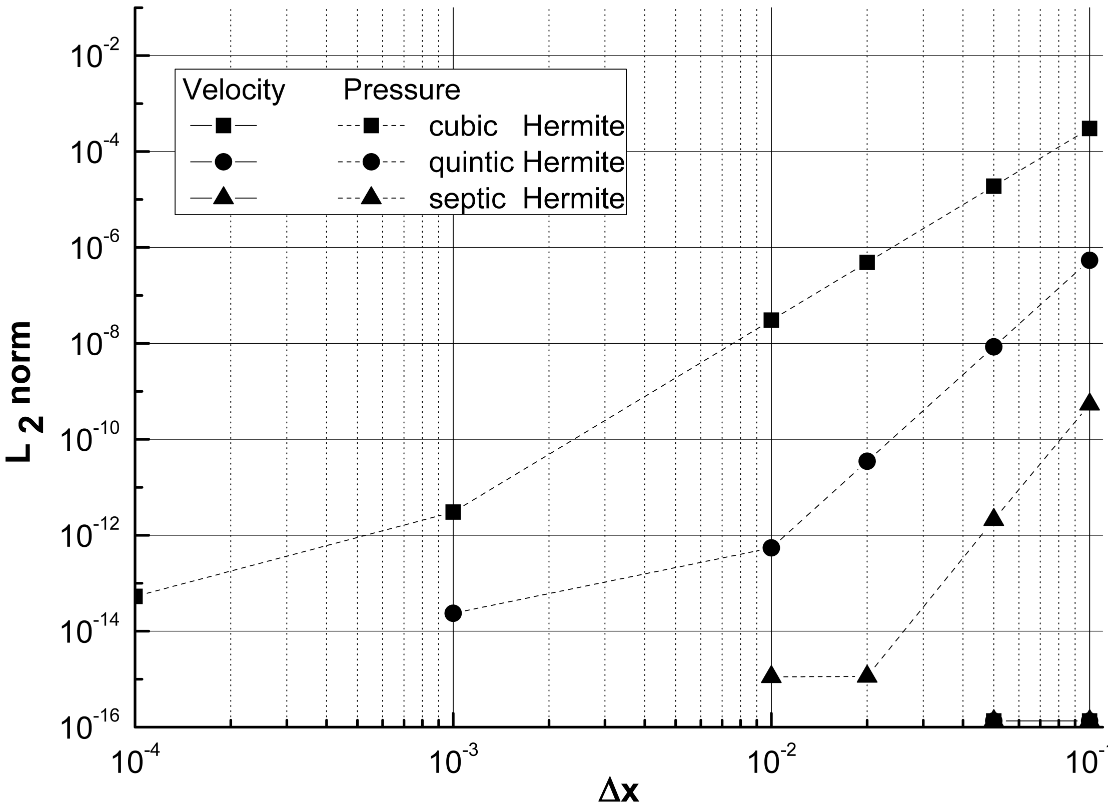

Figure 2: Case $\dot{m}$ linear and S_m exponential. Energy norm of velocity and pressure.

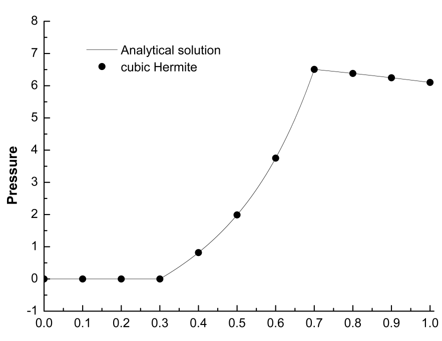

(a) Pressure field.

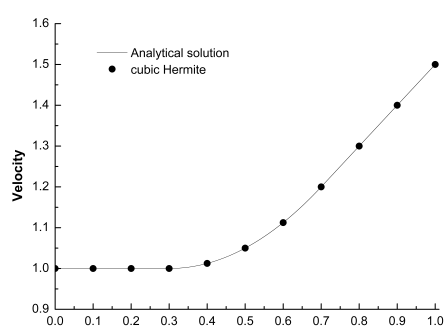

(b) Velocity field.

Figure 3: Case $\dot{m}$ linear and S_m exponential. Exact solution vs numerical solution with 9 internal nodes and 2 boundary nodes.

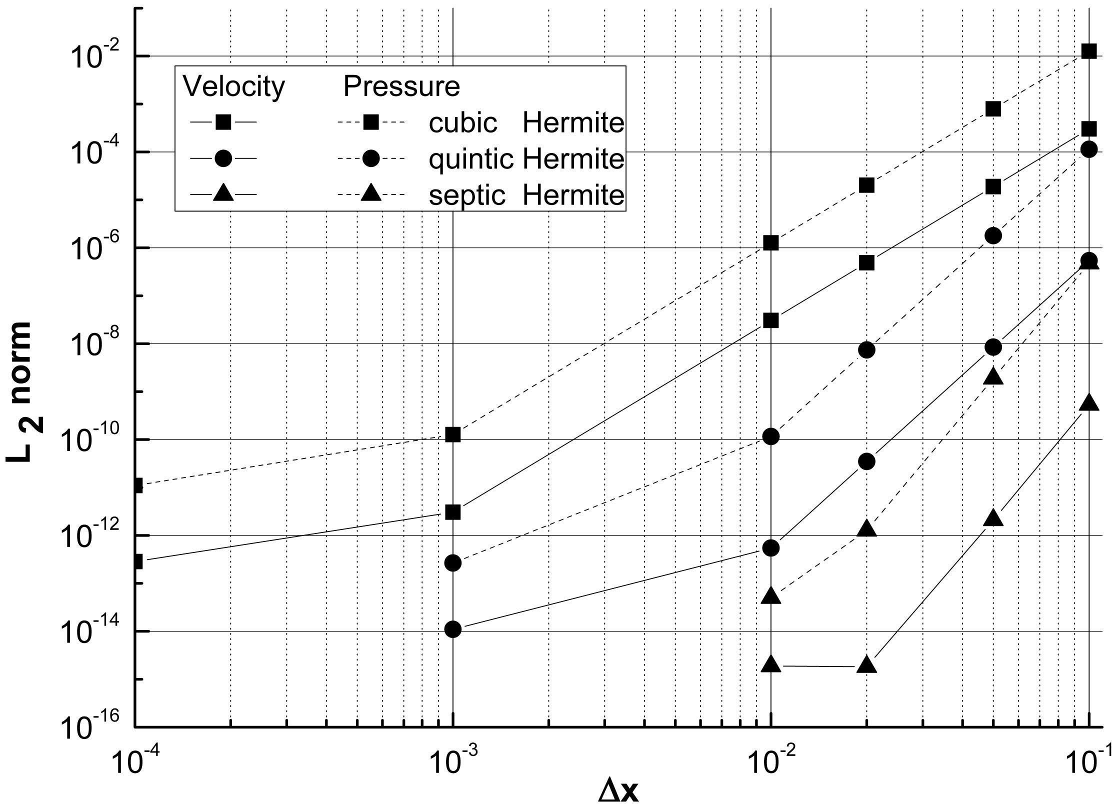

Figure 4: Case $\dot{m}$ exponential and S_m linear. Energy norm of velocity and pressure.

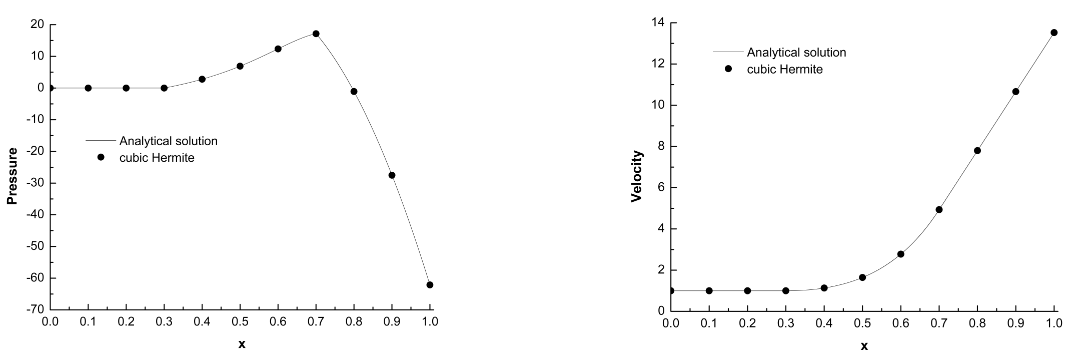

(a) Pressure field.

(b) Velocity field.

Figure 5: Case $\dot{m}$ exponential and S_m linear. Exact solution vs numerical solution with 9 internal nodes and 2 boundary nodes.

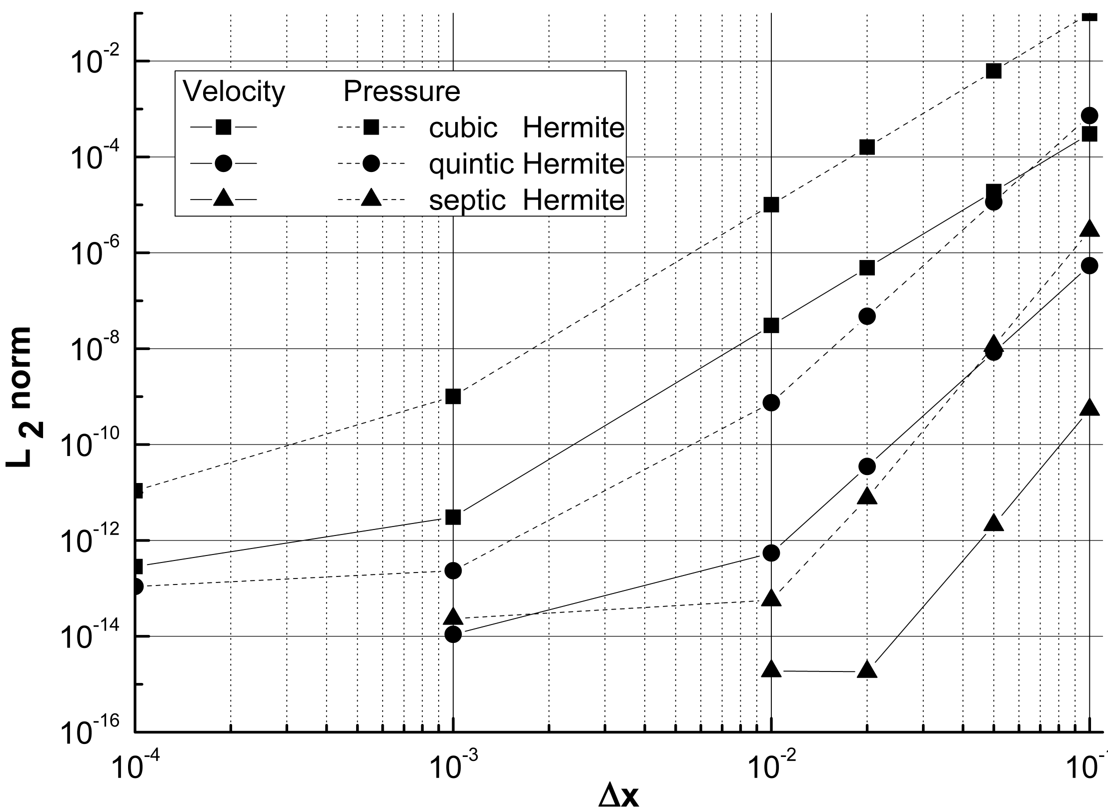

Figure 6: Case $\dot{m}$ exponential and S_m exponential. Energy norm of velocity and pressure.

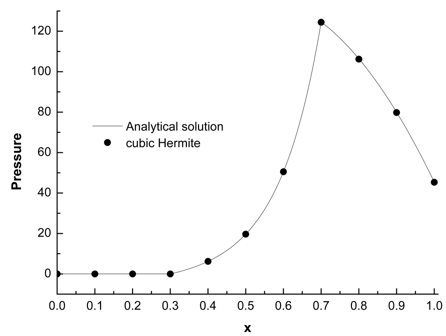

(a) Pressure field.

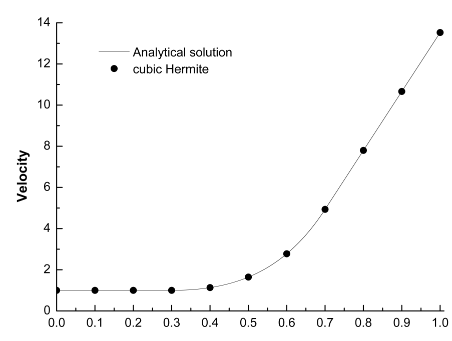

(b) Velocity field.

Figure 7: Case $\dot{m}$ and S_m exponential. Exact solution vs numerical solution with 9 internal nodes and 2 boundary nodes.